NEOPLASIA
www.neoplasia.com

Volume 12 Number 6 June 2010 pp. 464–475 464

Teriflunomide (Leflunomide) Promotes Cytostatic, Antioxidant, and Apoptotic Effects in Transformed Prostate Epithelial Cells: Evidence Supporting a Role for Teriflunomide in Prostate Cancer Chemoprevention[1]

Numsen Hail Jr., Ping Chen and Lane R. Bushman

Department of Pharmaceutical Sciences, University of Colorado Denver School of Pharmacy, Aurora, CO, USA

Abstract

Teriflunomide (TFN) is an inhibitor of *de novo* pyrimidine synthesis and the active metabolite of leflunomide. Leflunomide is prescribed to patients worldwide as an immunomodulatory and anti-inflammatory disease-modifying prodrug. Leflunomide inhibited the growth of human prostate cancer xenographs in mice, and leflunomide or TFN promoted cytostasis and/or apoptosis in cultured cells. These findings suggest that TFN could be useful in prostate cancer chemoprevention. We investigated the possible mechanistic aspects of this tenet by characterizing the effects of TFN using premalignant PWR-1E and malignant DU-145 human prostate epithelial cells. TFN promoted a dose- and time-dependent cytostasis or apoptosis induction in these cells. The cytostatic effects of TFN, which were reversible but not by the presence of excess uridine in the culture medium, included diminished cellular uridine levels, an inhibition in oxygen consumption, a suppression of reactive oxygen species (ROS) generation, S-phase cell cycle arrest, and a conspicuous reduction in the size and number of the nucleoli in the nuclei of these cells. Conversely, TFN's apoptogenic effects were characteristic of catastrophic mitochondrial disruption (i.e., a dissipation of mitochondrial inner transmembrane potential, enhanced ROS production, mitochondrial cytochrome *c* release, and cytoplasmic vacuolization) and followed by DNA fragmentation. The respiration-deficient derivatives of the DU-145 cells, which are also uridine auxotrophs, were markedly resistant to the cytostatic and apoptotic effects of TFN, implicating *de novo* pyrimidine synthesis and mitochondrial bioenergetics as the primary targets for TFN in the respiration-competent cells. These mechanistic findings advocate a role for TFN and mitochondrial bioenergetics in prostate cancer chemoprevention.

Neoplasia (2010) 12, 464–475

Introduction

Prostate cancer is one of the most frequently diagnosed tumors and the second leading cause of cancer death among men in the United States. Despite the routine use of diagnostic indicators for prostate cancer development (e.g., prostate-specific antigen screening), a high cure rate for localized disease, and an increased understanding of prostate cancer biology, most men who develop metastatic prostate cancer will succumb to this disease. Thus, it is clear that effective prostate cancer prevention strategies would spare many men the burden of diagnosis and treatment [1].

Cancer chemoprevention uses chemical agents to modulate carcinogenesis, thereby lowering the risk of developing invasive or clinically

Abbreviations: DCF, 2′,7′-dichlorofluorescein; DHODH, dihydroorotate dehydrogenase; $DiOC_6(3)$, 3,3′-dihexyloxacarbocyanine iodide; $\Delta\Psi_m$, mitochondrial inner transmembrane potential; FBS, fetal bovine serum; KGM, keratinocyte growth medium; Me_2SO, dimethyl sulfoxide; PI, propidium iodide; ρ^0, respiration-deficient cells lacking mitochondrial DNA; ROS, reactive oxygen species; TFN, teriflunomide

Address all correspondence to: Numsen Hail, Jr., University of Colorado Denver School of Pharmacy, C238-P15 Research 2, 12700 E 19th Ave, Room 3008, Aurora, CO 80045. E-mail: Numsen.Hail@UCDenver.edu

[1]This work was supported by funds provided by the National Cancer Institute (grant no. CA133901-01) and by the University of Colorado Denver School of Pharmacy.
Received 17 January 2010; Revised 22 March 2010; Accepted 24 March 2010

DOI 10.1593/neo.10168

significant disease. Cancer-chemopreventive agents typically intervene in the protracted promotion phase of carcinogenesis to inhibit or eliminate premalignant cells before they progress to malignancy. This can be accomplished by triggering cytostasis or apoptosis in the premalignant cells [2]. Given the indolent nature of prostate tumorigenesis, chemoprevention would seem to be a potentially highly effective approach for deferring malignancy [1].

Prostate tumorigenesis is coupled with an early metabolic switch in transformed prostate epithelial cells, which is attendant with a decrease in their citrate production through an increase in citrate oxidation by mitochondrial aconitase. This metabolic change functionally increases the mitochondrial bioenergetic capacity of the transformed prostate epithelial cells, which can provide a proliferative advantage that is required to establish tumorigenesis [3].

De novo pyrimidine synthesis is indispensable in rapidly proliferating cells to meet their increased demand for nucleic acid precursors, and this pathway is believed to be essential for aberrant cell proliferation after cell transformation [4]. Consequently, dihydroorotate dehydrogenase (DHODH, EC 1.3.99.11), an enzyme associated with mitochondrial electron transport and required for *de novo* pyrimidine synthesis [4], could be an important link between the enhanced mitochondrial bioenergetics and aberrant proliferation in transformed prostate epithelial cells.

Teriflunomide (TFN) is a redox silent coenzyme Q antagonist of DHODH and hence an inhibitor of *de novo* pyrimidine synthesis [5]. TFN's coenzyme Q–antagonizing effect is reportedly specific for dihydroorotate's oxidation to orotate by DHODH because in isolated rat liver, heart, and kidney mitochondria, the oxidation of succinate or NADH was only marginally suppressed (i.e., by roughly 33%) at relatively high concentrations (i.e., ≥100 μM) of the drug [6].

In vivo, TFN has well-known immunomodulatory and anti-inflammatory effects, and its prodrug leflunomide (Arava) has been prescribed to patients worldwide for the treatment of rheumatoid arthritis [7,8]. Leflunomide is converted nonenzymatically to TFN after oral ingestion, and plasma concentrations of TFN up to 300 μM have been attained in humans [7]. With a delayed elimination half-life of approximately 2 weeks, steady-state plasma concentrations (e.g., ~200 μM) of TFN can be reached roughly 14 to 20 weeks after the initiation of treatment with leflunomide [9], and adverse side effects are reportedly rare even after long-term therapy with leflunomide [8–10].

Leflunomide inhibited the growth of human prostate cancer xenographs in mice [11], and leflunomide or TFN promoted cytostasis and/or apoptosis in cultured cells [11–15]. These observations would soundly advocate a possible role for TFN in prostate cancer chemoprevention. Moreover, the probability that mitochondrial bioenergetics increases in transformed prostate epithelial cells [3] and the fact TFN functions as a coenzyme Q antagonist and anti-DHODH agent [5] would seemingly provide a prospective mechanistic basis for TFN-mediated prostate cancer chemoprevention. This study was undertaken to characterize the putative anticancer effects of TFN using premalignant and malignant prostate epithelial cells. The information presented here confirms that TFN can exploit the bioenergetic phenotype of these cells, which may be an important and novel means of engaging cytostasis or apoptosis and suppressing prostate tumorigenesis.

Materials and Methods

Cell Culture and Reagents

The premalignant PWR-1E [16] and malignant DU-145 [17] human prostate epithelial cells were kindly provided by Dr Rajesh Agarwal (University of Colorado Denver School of Pharmacy, Aurora, CO). The malignant LNCaP [17] and PC-3 [17] human prostate epithelial cells were kindly provided by Dr Reuben Lotan (University of Texas MD Anderson Cancer Center, Houston, TX). The PWR-1E cells were cultured in keratinocyte growth medium (KGM), consisting of keratinocyte basal medium supplemented with 100 ng/ml human recombinant epidermal growth factor, 0.4% bovine pituitary extract (all from Invitrogen Corporation, Carlsbad, CA), and 1 nM of the synthetic androgen R1881 (purchased from Perkin Elmer, Waltham, MA) as described previously [18]. For certain experiments, the indicated concentrations of uridine (purchased from Sigma-Aldrich Chemical Co, St Louis, MO) were added to the KGM to examine the effects of this pyrimidine nucleoside on the PWR-1E cells with or without TFN present.

The DU-145, LNCaP, and PC-3 cells were cultured in 1:1 Dulbecco's modified Eagle medium/Ham's F12 medium supplemented with 2% fetal bovine serum (FBS; Invitrogen). Where indicated, uridine (final concentration, 25 μM) was added to the culture medium of the DU-145 cells to examine its effects on TFN-induced cytostasis.

The respiration-deficient (i.e., ρ^0 cells lacking mitochondrial DNA) derivatives of DU-145 cells were isolated and characterized as described previously [18]. These cells were cultured in Dulbecco's modified Eagle medium containing 4.5 mg/ml D-glucose and 110 μg/ml pyruvate (Invitrogen) supplemented with 25 μM uridine and 2% FBS. All of the cell cultures were incubated at 37°C in humidified air containing 5% CO_2. Treatment with TFN was performed on subconfluent (i.e., ~40% confluent) cultures.

TFN (*N*-(4-trifluoromethylphenyl)-2-cyano-3-hydroxycrotoamide) was purchased from EMD Chemicals (Gibbstown, NJ). Dimethyl sulfoxide (Me_2SO), 2′,7′-dichlorofluorescin diacetate, dihydroethidium, and 3,3′-dihexyloxacarbocyanine iodide [$DiOC_6(3)$] were purchased from Sigma-Aldrich Chemical Co.

Nucleoside Quantitation in Cultured Cells

A modified version of a method published previously [19] was used to characterize the uridine, adenosine, and guanosine content in cultured cells. Briefly, approximately 2×10^6 cells were lysed in 500 μl of a 70% methanol/deionized water solution (vol./vol.). The cell debris was then removed through centrifugation (i.e., 1 minute at 12,000*g*). The resulting supernatant was passed through an anion exchange, solid-phase extraction cartridge (Waters QMA Accell Plus; Waters Division, Milford, MA), and the nucleotides were eluted from the cartridge with a 1-M KCl solution. Sweet potato type XA acid phosphatase (5 U; Sigma-Aldrich) in acetate buffer was added to the eluent to dephosphorylate the nucleotides. The samples were desalted and concentrated by a second solid-phase extraction that used a Phenomenex Strata X cartridge (Phenomenex, Torrance, CA). The methanol eluant from this extraction was dried under nitrogen gas and then reconstituted in 100 μl of deionized water.

A 5-μl injection volume and a mobile phase consisting of a phosphate buffer with an isocratic flow rate of 0.5 ml/min were passed through a Thermo Scientific Hypersil GOLD aQ 1.9-μm particle size, 2.1 × 100-mm ultra high-performance liquid chromatography column (Thermo Scientific, San Jose, CA) connected to a Waters Acquity ultra high-performance liquid chromatograph (Waters Division). The total uridine, adenosine, and guanosine in the samples was quantified using the characteristic UV absorption (i.e., 260 nm determined by photodiode array scanning from 210 to 400 nm) and retention time obtained from uridine, adenosine, and guanosine standards (Sigma-Aldrich) ranging from 5 to 500 ng (i.e., the amount injected on the column).

The standards were processed in the same manner as the cell samples (i.e., anion exchange, solid-phase extraction, and acid phosphatase digestion). The aforementioned concentration range for the nucleoside standards, analyzed using Waters Empore 2 software (Waters Division), produced a linear slope for both peak heights and peak areas (not shown).

Apoptosis Assay and Cell Cycle Analysis

Cellular DNA fragmentation was ascertained by using a hypotonic solution of propidium iodide (PI) [18]. The cell suspensions were analyzed for PI fluorescence intensity by flow cytometry. This procedure was also used to examine the cellular DNA content of viable cells relative to their cell cycle progression. The PI histograms were analyzed by ModFit LT version 3.2 software (Verity Software House, Inc, Topsham, ME), which modeled the cell cycle and provided the percentage of G_0/G_1, S, and G_2/M phase cells in each sample.

Assays for Determining Mitochondrial Inner Transmembrane Potential and Reactive Oxygen Species Production

Concurrent determinations of dissipation of mitochondrial inner transmembrane potential ($\Delta\Psi_m$) and reactive oxygen species (ROS) production were conducted as described previously [20]. Twenty minutes before the cells were harvested, $DiOC_6(3)$ and dihydroethidium were added directly to the culture medium (final concentrations of 40 nM and 5 μM, respectively). The cells were harvested and analyzed immediately for $DiOC_6(3)$ and ethidium fluorescence intensity by flow cytometry.

Flow Cytometry

The flow cytometry procedures were performed by a flow cytometer with CXP software (FC500; Beckman Coulter, Inc, Fullerton, CA). The experiments using flow cytometry were repeated at least two times. Approximately 10,000 cells were analyzed in each sample.

Continuous Monitoring of ROS Production in Cultured Cells

Short-term continuous intracellular ROS generation was measured using a microplate spectrofluorimeter assay [18]. Fluorescence emission at 538 nm (representing the oxidation of dichlorofluorescin to 2′,7′-dichlorofluorescein [DCF]) after excitation at 485 nm was measured at time 0 (immediately after the addition of 2′,7′-dichlorofluorescin diacetate) and subsequently at 30-minute intervals during a 150-minute period using a dual-scanning microplate spectrofluorimeter (SpectraMax Gemini EM; Molecular Devices, Sunnyvale, CA).

Measurement of Oxygen Consumption in Cultured Cells

Oxygen consumption was measured polarographically using a Clark-type oxygen electrode and monitor (Model 5300A Biological Oxygen Monitor; Yellow Spring Instrument Co, Yellow Springs, OH) [18]. The oxygen consumption measurements were recorded and analyzed using Logger Pro version 3.0 software (Vernier Software and Technology, Beaverton, OR). The oxygen consumption rates (nmol of O_2/min) were normalized for 10^6 cells.

Assessment of Cytosolic Cytochrome c

Extramitochondrial cytochrome *c* was determined as described previously [18]. Briefly, the PWR-1E cells were treated for 6 hours with 50, 100, or 200 μM TFN or with an equal volume of the vehicle Me_2SO. The cells were harvested, washed once with 1 ml of phosphate-buffered saline, and gently vortexed for 30 seconds in 80 μl of ice-cold cell permeabilization buffer. The cell suspensions were centrifuged at 12,000*g* for 5 minutes at 4°C to separate the soluble protein fraction from the permeabilized cells. The supernatant proteins (~50 μl) were subjected to electrophoresis in a SDS–polyacrylamide slab gel and were evaluated using immunoblot analysis.

Immunoblot Analysis

Cellular proteins were characterized as described previously [18]. The cells were washed with ice-cold phosphate-buffered saline, harvested by trypsinization, and resuspended in lysis buffer that was supplemented with a protease inhibitor cocktail (Sigma-Aldrich). The samples (~30 μg each) were separated through electrophoresis followed by transfer to a nitrocellulose membrane (Bio-Rad Laboratories, Hercules, CA). The membranes were probed with the antibodies for the human proteins DHODH (purchased from Sigma-Aldrich), cytochrome *c*, or β-actin (both purchased from Santa Cruz Biotechnology, Santa Cruz, CA). The binding of the primary antibody was detected with a horseradish peroxidase–linked secondary antibody using an enhanced chemiluminescence kit (Amersham Biosciences Corp, Piscataway, NJ). The DHODH and β-actin immunoblots were subjected to densitometric analysis using ImageJ software (National Institutes of Health, Bethesda, MD). The DHODH band intensity was normalized as a percentage of the loading control β-actin.

Statistical Analyses

The statistical significance between the means of two groups or more was determined using a two-sided, unpaired *t* test or a one-way analysis of variance with the Dunnett post test, respectively (GraphPad InStat version 3.0 software; GraphPad Software, Inc, San Diego, CA). Where indicated, the results are expressed as the mean value of triplicate samples ± SD (error bars). All means ± SD were calculated with Microsoft Excel 2003 SP2 software (Microsoft Corporation, Seattle, WA). In all statistical analyses, the results were considered significant for $P < .05$.

Results and Discussion

DHODH Protein Expression Parallels the Oxygen Consumption by Premalignant and Malignant Prostate Epithelial Cells

It has been estimated that less than 1% of the normal epithelial cells in the adult human prostate undergo routine cell division [21]. This may explain why DHODH expression and biochemical activity in normal prostate tissues were negligible compared with those observed in transformed cells such as Ehrlich ascites tumor cells [22]. DHODH is located in the inner mitochondrial membrane where it serves as the rate-limiting enzyme in the *de novo* pathway of pyrimidine synthesis [4]. Coenzyme Q is the proximal electron acceptor for dihydroorotate's oxidation to orotate by DHODH. Oxygen functions as the ultimate electron acceptor for this reaction through electron transfer at cytochrome *c* oxidase (i.e., complex IV). In this scenario, dihydroorotate acts as a reducing equivalent like NADH or succinate to modulate mitochondrial respiration (Figure 1*A*).

There are currently no reported assessments of DHODH expression or activity in transformed human prostate epithelial cells. We examined DHODH expression in the DU-145, LNCaP, PC-3, and PWR-1E cells. Among the premalignant PWR-1E and malignant DU-145, LNCaP, and PC-3 prostate epithelial cells, the PWR-1E and LNCaP cells had roughly twofold higher DHODH protein expression compared with the DU-145 and PC-3 cells (Figure 1*B*). The oxygen consumption (used

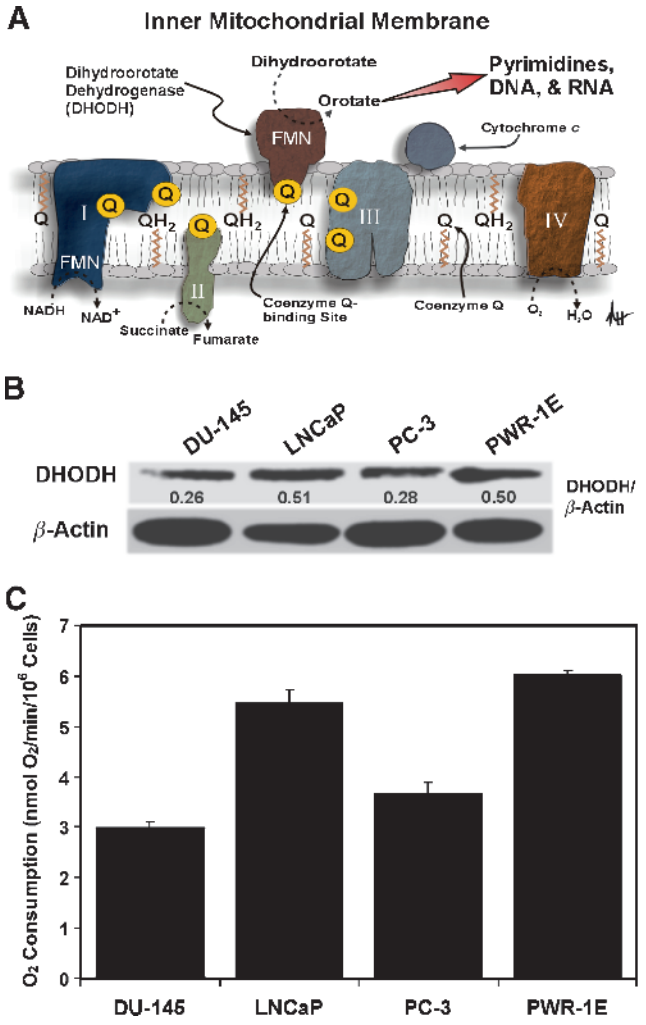

Figure 1. An assessment of DHODH expression and oxygen consumption in transformed prostate epithelial cells. (A) A diagrammatic depiction of DHODH in the inner mitochondrial membrane illustrating its role in mitochondrial bioenergetics and *de novo* pyrimidine synthesis. Please refer to the text for additional details (*I* indicates complex I; *II*, complex II; *III*, complex III; *IV*, complex IV; *FMN*, flavin mononucleotide). (B) An immunoblot analysis of DHODH expression for the DU-145, LNCaP, PC-3, and PWR-1E cells. The DHODH band intensity was normalized as a percentage of the loading control β-actin using ImageJ software. (C) The oxygen consumption rates (nmol of O_2/min) were determined for approximately 10^6 cells.

as a surrogate indicator of mitochondrial bioenergetics) by the PWR-1E and LNCaP cells was also nearly twice that measured in an equal number of DU-145 or PC-3 cells (Figure 1*C*), indicating that DHODH expression was possibly interrelated with mitochondrial bioenergetics in the PWR-1E and LNCaP cells.

Interestingly, the PWR-1E [16] and LNCaP [23] cells are responsive to androgens for their proliferation, which has also been implicated with enhanced mitochondrial bioenergetics in LNCaP cells [23]. Furthermore, both PWR-1E [18] and LNCaP [24] cells have been characterized as being more oxidative, with respect to their bioenergetic capacity, than the DU-145 and/or PC-3 cells. Premalignant cells represent a very early stage of cancer development and are therefore the envisioned target for cancer chemoprevention [2]. Consequently, we chose to further evaluate the effects of TFN on the premalignant PWR-1E and malignant DU-145 cells to determine whether their relative DHODH expression and/or bioenergetic phenotype would affect sensitivity to this agent.

TFN Causes a Dose- and/or Time-Dependent Suppression of Cell Proliferation, Reduction in Cellular Uridine, Cell Cycle Arrest, and Morphological Changes in PWR-1E and DU-145 Cells

Short-term (e.g., 24-72 hours) exposures to low micromolar (e.g., 10-200 μM) concentrations of leflunomide or TFN can promote cytostasis (i.e., cause G_0/G_1-phase [12,13] or S-phase [11,25] cell cycle arrest) and/or apoptosis [12,14,25] in hematopoietic cells including normal mitogen-stimulated human T lymphocytes [13], normal human mast cells [14], human myeloma cells [12], human chronic lymphocytic leukemia cells [25], and murine leukemia cells [15], as well as transformed murine fibroblasts [11]. However, no mechanistic data that would propose how TFN could function as a potential cytostatic/apoptogenic cancer-chemopreventive agent against transformed prostate epithelial cells have emerged.

We exposed the PWR-1E cells to increasing micromolar concentrations of TFN for 24 hours and examined cell number as an indicator of proliferation or cytostasis. As illustrated in Figure 2*A*, increasing the concentration of TFN promoted a concomitant decrease in cell number in these populations relative to the Me_2SO-treated controls. The 50-, 100-, and 200-μM concentrations of TFN seemed to be equally effective in triggering a seemingly complete inhibition of cell proliferation after 24 hours because the doubling time for these cells was roughly 26 hours. Even after a 48-hour exposure to 25 μM TFN, we observed a reduction greater than 50% in cell number compared with that in the control (not shown).

A 24-hour exposure to 25, 50, or 100 μM TFN did not seem, through microscopic examination, to be cytotoxic to the PWR-1E cells. However, during a 24-hour exposure to 200 μM, TFN apoptotic morphology [18] (i.e., cytoplasmic vacuolizations, cell shrinkage and rounding, and an obvious increase in the number of floating cells in the culture medium compared with the Me_2SO-treated control cells; not shown) could be observed in many of the PWR-1E cells. Consequently, we decided to focus on 50 μM TFN to further investigate the cytostatic effects of this agent. To this end, we observed a time-dependent decrease in cell number relative to the respective controls in both the PWR-1E and DU-145 cells exposed to TFN for 24 or 48 hours (Figure 2*B*). The cytostatic effect of TFN was similar in the premalignant and malignant cells, indicating that their relative DHODH expression and oxygen consumption did not profoundly affect their short-term sensitivity to this agent. Moreover, both the DU-145 and PWR-1E cells exhibited a similar time-dependent decrease in cellular uridine levels after a 12- and 24-hour exposure to 50 μM TFN (Figure 2*C*). The adenosine and guanosine purine nucleoside levels remained essentially unchanged in these cells, relative to their respective controls, during this treatment (not shown). We examined the DHODH expression in the DU-145 and PWR-1E cells after a 24-hour exposure to 50 μM TFN and found no change in this protein relative to the Me_2SO-treated control cells (not shown).

Exposure to 50 μM TFN also caused a time-dependent accumulation of both the DU-145 and PWR-1E cells in the S phase of the cell cycle compared with the Me_2SO-treated control cells (Figure 2*D*). This S-phase arrest accounted for roughly 80% of the treatment populations after the 48-hour exposure to TFN. A summary of the cell cycle distributions for triplicate samples obtained from these 24- and 48-hour exposures to TFN or Me_2SO is presented in Figure 2*E*.

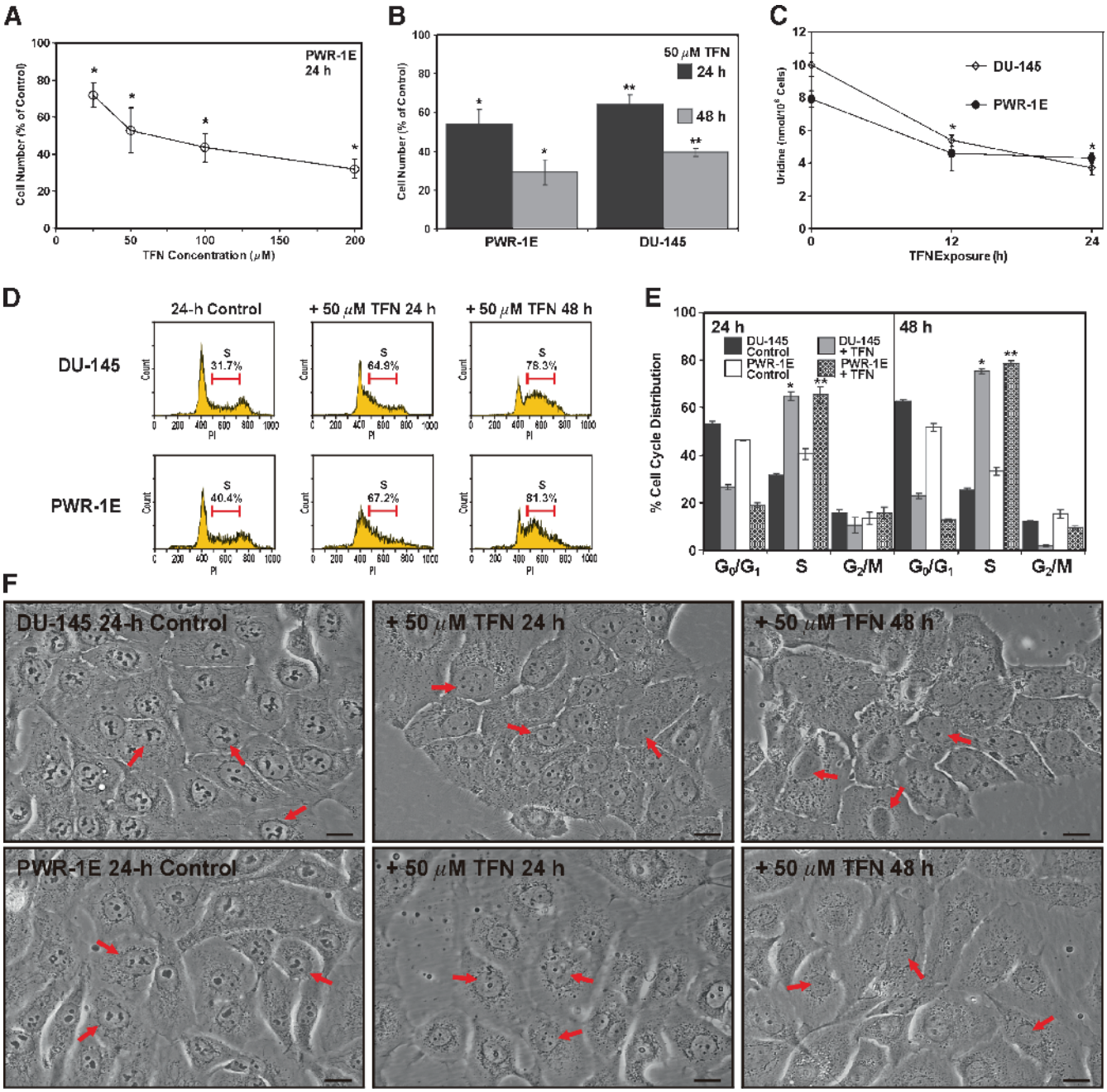

Figure 2. TFN inhibits proliferation and decreases cellular uridine levels in PWR-1E and DU-145 cells. (A) The PWR-1E cells were treated for 24 hours with the indicated concentrations of TFN or an equal volume of the vehicle Me_2SO (control) dissolved in fresh culture medium. The cells were harvested and counted with a hemacytometer. The relative cell number in the TFN-treated populations is presented as a percentage of the 24-hour control. $P < .001$ compared with control. (B) The PWR-1E and DU-145 cells were cultured, harvested, and counted as described in panel (A) after 24- and 48-hour exposures to 50 μM TFN or Me_2SO (control). *$P < .01$ compared with the respective PWR-1E controls; **$P < .01$ compared with the respective DU-145 controls. (C) An assessment of the uridine levels in the DU-145 and PWR-1E cells after exposure to 50 μM TFN for the indicated times or Me_2SO (control, 0-hour TFN exposure). *$P < .01$ compared with the 0-hour DU-145 or PWR-1E control. (D) Representative PI (DNA) histograms for the treatments described in panel (B). The percentages of S-phase cells are presented above the histograms. (E) A summary of the cell cycle analyses for the treatments described in panel (B). *$P < .001$ compared with the respective DU-145 controls; **$P < .001$ compared with the respective PWR-1E controls. (F) DU-145 and PWR-1E cells were imaged at the indicated times after treatment with 50 μM TFN or Me_2SO (control). The arrows in the differential interference contrast images point to the cell nucleus. Scale bars, 18 μm.

When viewed with a microscope, the DU-145 and PWR-1E cells exposed to 50 μM TFN for 24 or 48 hours appeared morphologically flatter, were less pleomorphic, had greater cell-to-cell contact, and exhibited a granular cytoplasm compared with their respective control cells (Figure 2*F*). There was also an obvious reduction in the size and number of the nucleoli in the nuclei of these cells (Figure 2*F*, *arrows*). A similar depletion of nucleoli has been observed in hepatocytes derived from rats deprived of dietary nucleotides [26]. Together, these

results demonstrated that the short-term cytostatic effect of TFN resulted from directly decreasing *de novo* pyrimidine synthesis and subsequent DNA synthesis in the PWR-1E and DU-145 cells.

Short-term Exposure to TFN Inhibits Mitochondrial Oxygen Consumption and ROS Production in Premalignant and Malignant Prostate Epithelial Cells

The modulation of *de novo* pyrimidine synthesis by TFN in the transformed prostate epithelial cells should also diminish the overall mitochondrial function in these cells. Indeed, a short-term 4-hour exposure to TFN reduced the oxygen consumption by approximately 20% in the DU-145 cells and by roughly 30% in the PWR-1E cells (Figure 3*A*). We have previously reported that the oxygen consumption in these cells is sensitive to cyanide, which demonstrated that this cellular biochemical feature was associated with mitochondrial respiration [18].

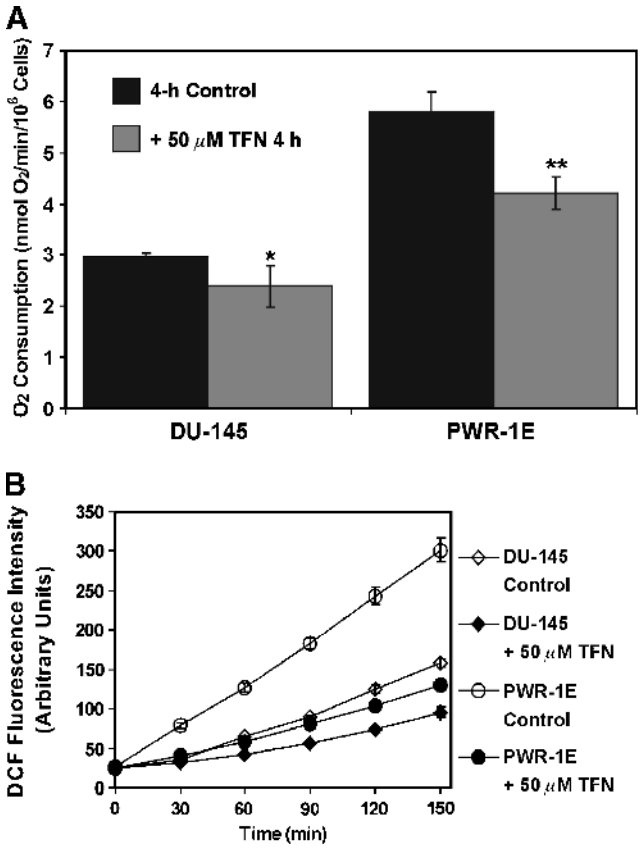

Figure 3. Short-term exposure to TFN suppresses oxygen consumption and ROS production in PWR-1E and DU-145 cells. (A) The DU-145 and PWR-1E cells were treated with Me_2SO (control) or 50 μM TFN in fresh culture medium for 4 hours and examined for oxygen consumption as described in Figure 1*C*. *$P < .05$ compared with the DU-145 control; **$P < .01$ compared with the PWR-1E control. (B) PWR-1E and DU-145 cells cultured in six-well tissue culture plates were exposed to 50 μM TFN or to an equal volume of the vehicle Me_2SO (control) as described in panel (A). The medium was removed and replaced with Krebs-Ringer buffer containing 10 μg/ml 2′,7′-dichlorofluorescin diacetate. Fluorescence emission at 538 nm (representing DCF production) was measured immediately after mixing (time 0) and subsequently at 30-minute intervals during a 150-minute period. The spectrofluorimeter preformed 12 fluorescence measurements per well and provided the mean DCF fluorescence value.

If DHODH and *de novo* pyrimidine synthesis were constitutively active in these cells as the decrease in cellular uridine levels (Figure 2*C*) and the inhibition of oxygen consumption (Figure 3*A*) by TFN indicated, this should affect not only their rate of proliferation (Figure 2*B*) but also their endogenous mitochondrial ROS production [27]. This enhanced mitochondrial ROS production could act as a feed-forward mechanism for tumor promotion in the prostate [28]. As shown in Figure 3*B*, a 4-hour exposure to TFN also suppressed the oxidation of 2′,7′-dichlorofluorescin to DCF in both the DU-145 and PWR-1E cells. There was nearly a 50% reduction in the rate of ROS production between 30 and 150 minutes in the DU-145 cells and roughly a 65% reduction in the rate of ROS production during the same period in the PWR-1E cells. Thus, TFN could be broadly classified as an antioxidant in these cells.

Excess Uridine Is Ineffective against TFN-Induced Cytostasis

We treated the PWR-1E cells for 48 hours with 50 μM TFN, replaced their culture medium, and examined the change in cell number and the percentage of S-phase cells in the pretreated cell populations during the subsequent 3 days to determine whether the acute cytostatic effect of TFN could be reversed. As shown in Figure 4*A*, the fresh TFN-free culture medium encouraged cell proliferation, albeit seemingly slower than we normally observed in the PWR-1E cells, as evidenced by an increase in the cell number relative to the cells exposed to TFN for 48 hours. Likewise, the release from TFN allowed a concomitant decrease in the S-phase cells in the cell cycle as shown in Figure 4*B*. The slow time-dependent recovery from the short-term cytostatic consequences of the TFN treatment in these cells could have resulted from a nonspecific off-target effect. It is also possible that the disassociation of TFN from DHODH in the PWR-1E cells was a protracted process because TFN exhibits a high binding affinity for proteins *in vivo* and *in vitro* [8].

Pyrimidines may be salvaged from the extracellular fluid to meet some degree of cellular demand [4]. Although it has relatively low bioavailability [29], uridine is reportedly the most abundant salvageable pyrimidine nucleoside *in vivo* [29]. The uridine concentration of human plasma is roughly 5 μM [29]. This concentration is estimated to be approximately five to six times lower than those in liver, kidney, and spleen tissues that typically contain the highest levels of uridine [29]. *In vitro*, approximately 1 to 5 μM uridine is reportedly present in tissue culture medium provided the medium is supplemented with 5% to 10% nondialyzed FBS [30].

We wanted to determine whether uridine added to the serum-free KGM of the PWR-1E cells would influence proliferation in these cells. A 48-hour exposure to 5, 10, or 25 μM uridine had no obvious effect on the number of PWR-1E cells compared with their untreated control cells, whereas a 48-hour exposure to 50 or 100 μM uridine promoted a mild (i.e., roughly 20%) suppression of PWR-1E cell proliferation (Figure 5*A*). Interestingly, enterocyte proliferation *in vitro* was also reportedly suppressed by supraphysiological (e.g., >50 μM) concentrations of uridine [31].

We next investigated the effects of 25 μM uridine on TFN-induced cytostasis in the PWR-1E cells. Fresh KGM with or without uridine was added to the PWR-1E cell cultures at the time of TFN treatment, and these cells were monitored for 48 hours. As shown in Figure 5*B*, without uridine present, the TFN-treated PWR-1E cells exhibited the same morphological features that were illustrated previously in Figure 2*F*. Surprisingly, when 25 μM uridine was present along with 50 μM TFN, these cells exhibited similar apoptotic morphological

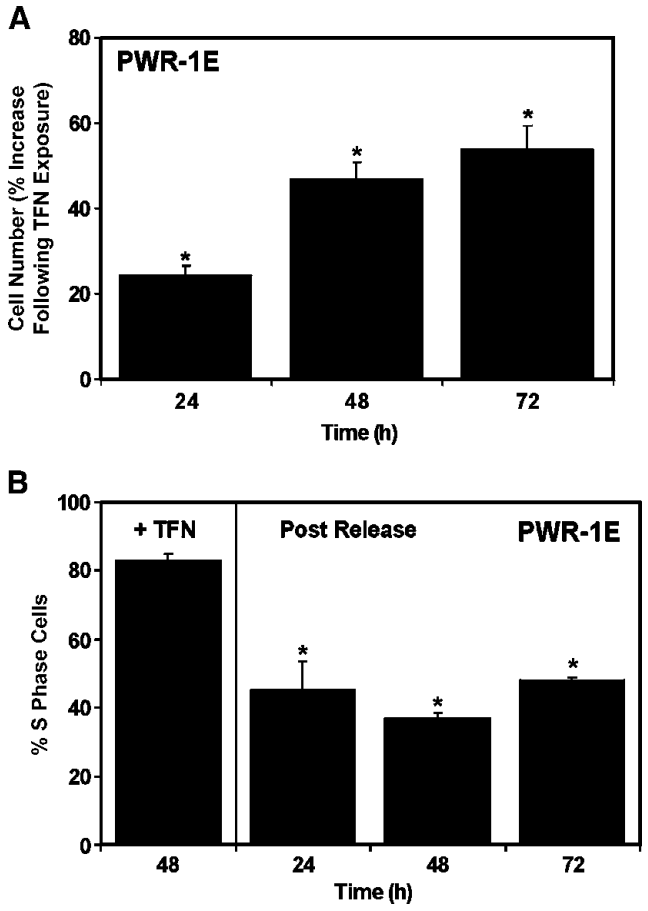

Figure 4. Cessation of TFN treatment reverts cytostasis in PWR-1E cells. The PWR-1E cells were treated for 2 days with 50 μM TFN dissolved in fresh KGM. The cultures were examined for cell number (as described in Figure 2*A*) and percent S-phase cells (as described in Figure 2*D*). In the remaining plates, the cells received fresh KGM after the initial 48-hour exposure to TFN. These cultures were examined for cell number (A) and percent S-phase cells (B) as described previously during the next 3 days. *$P < .01$ compared with the PWR-1E cell number after the 48-hour TFN exposure (A); *$P < .01$ compared with the S-phase cell population resulting from the initial 48-hour exposure to TFN (B).

changes described previously for the PWR-1E cells exposed to 200 μM TFN. Specifically, we observed the progressive development of cytoplasmic vacuolizations, cell shrinkage and rounding, nuclear condensation, cell fragmentation, and an obvious increase in the number of floating cells in the culture medium (not shown) of the PWR-1E cells treated with uridine and TFN compared with the cells treated with TFN alone or the Me_2SO-treated control cells (Figure 5*B*). There was also a time-dependent increase in the number of hypoploid apoptotic cells in the PWR-1E cells cotreated with uridine and TFN that constituted approximately 40% of the treatment population after 48 hours (Figure 5*C*). The basis for the acute cytotoxicity of the TFN and uridine combination in the PWR-1E cells is unknown.

We have previously isolated and characterized DU-145 ρ^0 cells. These cells, by the nature of their respiration deficiency, are uridine auxotrophs. The doubling time for the DU-145 ρ^0 clones is approximately 56 hours, whereas the parental DU-145 cells double in approximately 27 hours without the need for supplemental uridine in their culture medium [18]. Moreover, we detected no difference in the proliferation rate of the DU-145 ρ^0 clones after a 4-day culture in medium containing 25, 50, 100, or 200 μM uridine (not shown), suggesting that the uridine concentration alone could not regulate proliferation in these cells.

We have also isolated ρ^0 clones from cutaneous squamous cell carcinoma cells [32] that exhibit slow-growth characteristics similar to the DU-145 ρ^0 clones. The distinct growth characteristics displayed by the parental cells and their ρ^0 clones affirm that some aspects of mitochondrial bioenergetics augmented the rate of cell proliferation in the parental cells [18]. The isolation of the ρ^0 clones was not a rapid process. It typically required approximately 8 to 10 weeks to deplete the mitochondrial DNA and adapt the ρ^0 clones to grow, albeit slowly, in culture medium containing high glucose, uridine, and pyruvate. In effect, the up-regulation of a uridine salvage mechanism in the ρ^0 clones was coupled with a severe long-term impairment of mitochondrial bioenergetics. As a result, the growth characteristics of the ρ^0 cells *in vitro* potentially emulate tumor cell growth under hypoxic conditions *in vivo*, which is commonly observed in solid tumors or in metastatic tumor sites such as the bone marrow [18].

We cultured the DU-145 cells and their ρ^0 counterparts in medium containing 25 μM uridine and assessed the effects of TFN on their proliferation, cell cycle distribution, and cellular morphology. As illustrated in Figure 6*A*, the DU-145 cells exposed to TFN in the presence of 25 μM uridine exhibited essentially the same degree of growth suppression caused by TFN without supplemental uridine in the culture medium (Figure 2*B*). Similar observations have been reported for human chronic lymphocytic leukemia cells exposed to TFN with or without uridine present in the culture medium [25]. Interestingly, normal mitogen-stimulated human T lymphocytes [13], normal human mast cells [14], human myeloma cells [12], murine leukemia cells [15], and transformed murine fibroblasts [11] examined for growth suppression and/or apoptosis induction by TFN or leflunomide were able to avert these effects if uridine was added to their culture medium. The apparent ability of the pyrimidine salvage pathway to overcome TFN's effects on cell proliferation and/or apoptosis induction in the aforementioned cells may be dependent on cell type. No apparent cytotoxic effects of the TFN-uridine combination were detected in the DU-145 cells (not shown). TFN also a caused a slight antiproliferative effect in the ρ^0 clones, which, although statistically significant after 48, 72, and 96 hours, did not emulate the short-term biological effect of TFN observed in the parental cells (Figure 6*A*).

The presence of uridine could not repress the 48-hour S-phase cell cycle arrest caused by 50 μM TFN in the DU-145 cells. This treatment had a different effect on the cell cycle distribution of the ρ^0 clones. The ρ^0 clones appeared to have slightly less S-phase cells after 48-, 72-, and 96-hour exposures to TFN (Figure 6*B*) with a concomitant small accumulation of cells in the G_0/G_1 phase of the cell cycle (not shown). This seemingly off-target effect could not be intimately associated with the antiproliferative activity of TFN in the PWR-1E or parental DU-145 cells because, if this were the case, we would not expect to detect the profound accumulation of S-phase cells after the short-term (i.e., 24 or 48 hours) exposures to TFN. Furthermore, the ρ^0 clones exposed to 50 μM TFN in the presence of 25 μM uridine for 96 hours were indistinguishable from their Me_2SO-treated (i.e., control) counterparts as evidenced by their morphological (Figure 6*C*), nuclear (Figure 6*C*, *arrows*), and cell cycle (Figure 6*C*, *insets*) criteria. Conversely, we observed conspicuous morphological (e.g., cell flattening), nuclear (i.e., a marked reduction in the size and number of the nucleoli in the nuclei of these cells), and cell cycle alterations (i.e.,

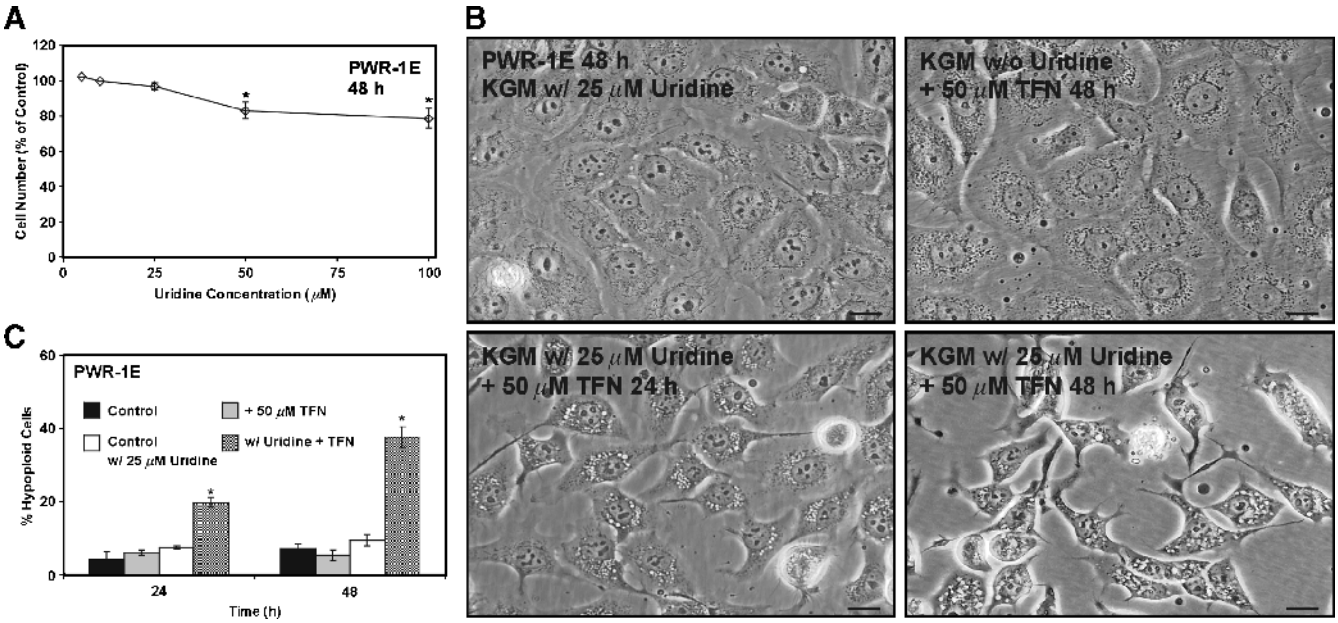

Figure 5. Uridine combined with TFN promotes cytotoxicity in PWR-1E cells. (A) The PWR-1E cells were cultured in KGM (control) or KGM with 5, 10, 25, 50, or 100 μM uridine for 2 days. The cells were harvested and counted as described in Figure 2*A*. The relative cell number in the uridine-treated cell populations is presented as a percentage of the untreated 48-hour control population. *$P < .01$ compared with the untreated control. (B) DIC micrographs showing PWR-1E cells cultured in KGM containing 25 μM uridine for 48 hours, the PWR-1E cells exposed to 50 μM TFN for 48 hours in KGM without uridine, and the PWR-1E cells exposed to 25 μM uridine and 50 μM TFN for 24 and 48 hours. Scale bars, 18 μm. (C) A summary of the hypoploid cells in the treatment populations described in panel (B). Me_2SO was included in the control treatments without or with 25 μM uridine. *$P < .001$ compared with the TFN treatment alone.

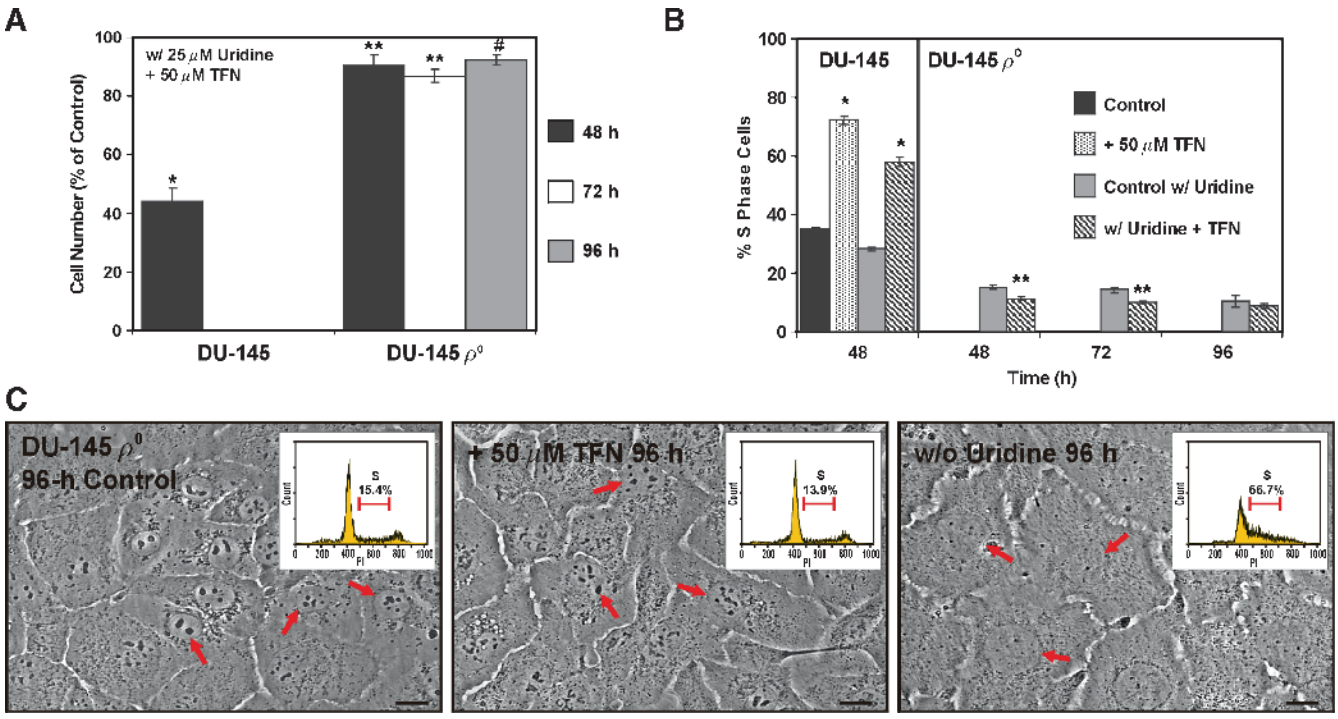

Figure 6. DU-145 uridine auxotrophs oppose the acute cytostatic effects of TFN. (A) DU-145 cells and their ρ^0 clones were cultured for the indicated times in medium containing 25 μM uridine and 50 μM TFN or Me_2SO (control). The cells were harvested and counted as described in Figure 2*A*. *$P < .001$ compared with the DU-145 control; **$P < .01$ or $^{\#}P < .05$ compared with the ρ^0 control. (B) The percent S-phase cells in the indicated treatment populations was determined as described in Figure 2*D*. *$P < .001$ for the TFN-treated DU-145 cells compared with the respective control without or with uridine; **$P < .01$ for the TFN-treated ρ^0 clones compared with the ρ^0 control with uridine present. (C) The ρ^0 clones were imaged 96 hours after treatment with 50 μM TFN, Me_2SO (control), or culture without uridine. The arrows in the DIC images point to the cell nucleus. Scale bars, 18 μm. The insets in the DIC images are representative PI (DNA) histograms for the treatments indicated. The percent S-phase cells in each treatment population was determined as described in panel (B).

S-phase cell cycle arrest) in the ρ^0 clones deprived of uridine for 96 hours (Figure 6*C*).

Together, the results presented in Figures 1 to 6 clearly demonstrate that 1) bioenergetics and the *de novo* pathway for pyrimidine synthesis were apparently crucial for the enhanced rate of cell proliferation in the PWR-1E and parental DU-145 cells compared with the DU-145 ρ^0 clones; 2) bioenergetics and the *de novo* pathway for pyrimidine synthesis contributed to ROS production in the PWR-1E and DU-145 cells; 3) excess uridine could not reverse the short-term cytostatic effects of TFN in the PWR-1E or DU-145 cells, demonstrating that *de novo* pyrimidine synthesis and pyrimidine salvage were not functionally interchangeable as a means of sustaining the typical rate of cell proliferation in these cells; 4) mitochondrial bioenergetics was required for the effects of TFN in the respiring cells; 5) pyrimidine deficiency was associated with the conspicuous reduction in the size and number of the nucleoli in the nuclei of the PWR-1E and DU-145 cells exposed to TFN or the ρ^0 clones deprived of uridine; and 6) pyrimidine deficiency was a central determinant in the S-phase cell cycle arrest detected in the ρ^0 clones deprived of uridine as well as the DU-145 and PWR-1E cells exposed to TFN.

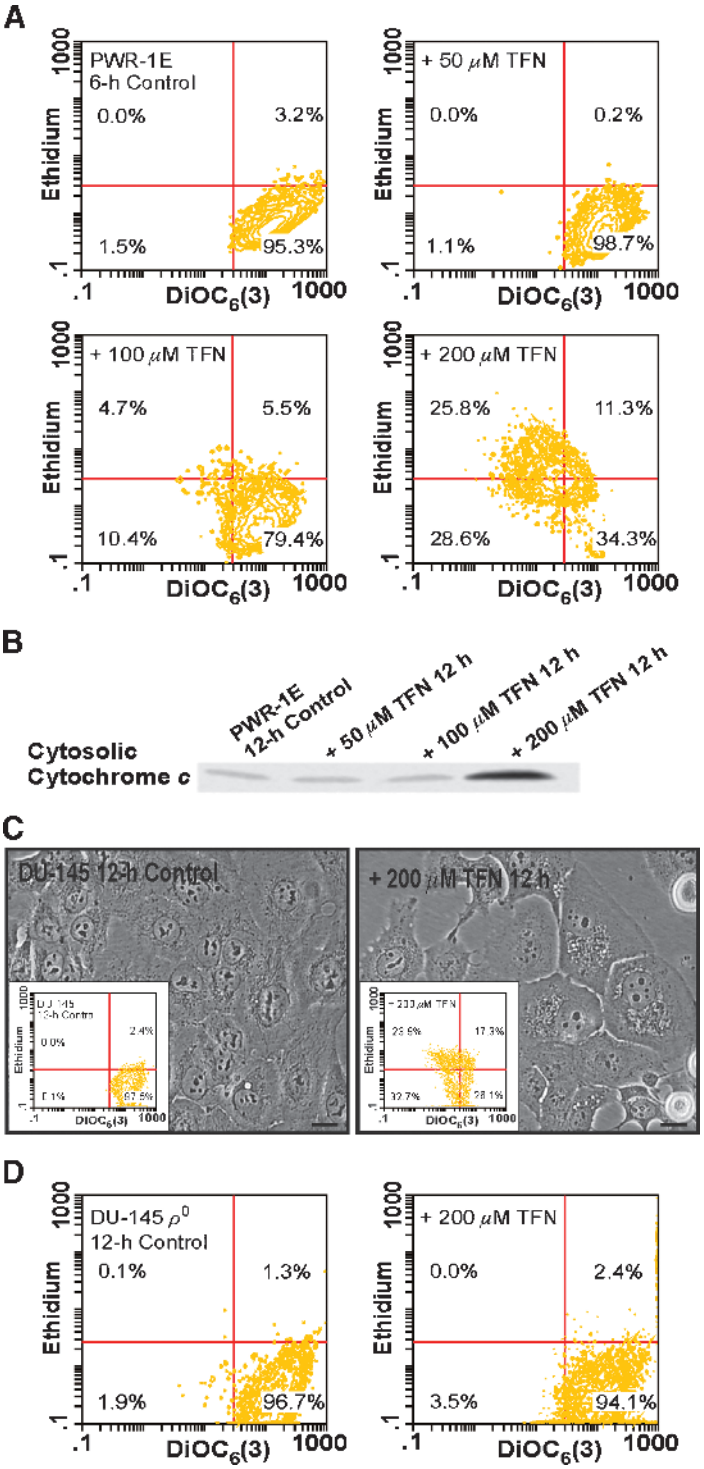

TFN-Induced Apoptosis Is Associated with Catastrophic Mitochondrial Disruption in PWR-1E and DU-145 Cells

The previous data revealed that TFN modulated *de novo* pyrimidine synthesis, and essentially mitochondrial function, to trigger cell cycle arrest/cytostasis in the premalignant and malignant prostate epithelial cells. Because we also observed a dose-dependent cytotoxic effect for 200 μM TFN in the PWR-1E cells, it was certainly possible that this putative DHODH inhibitor and coenzyme Q antagonist was causing an irreversible catastrophic effect to the cell's mitochondria to trigger cell death. In fact, leflunomide at concentrations ≥100 μM not only markedly reduced the pyrimidine pools in mitogen-stimulated human T lymphocytes but also conspicuously depleted the ATP and GTP pools in these cells. These effects essentially caused a complete metabolic collapse in these cells, which could account for some of the ancillary effects, such as kinase inactivation [11,14,15], caused by high concentrations of leflunomide or TFN *in vitro* [13]. Therefore, we conjectured that higher (e.g., >100 μM) *in vitro* concentrations of TFN could promote a profound disruption of mitochondrial function in the transformed prostate epithelial cells as well.

Many putative cancer-chemopreventive agents can alter mitochondrial function to trigger apoptosis in transformed cells [33], and several of the chemopreventive agents we have examined previously, including the synthetic retinoid *N*-(4-hydroxyphenyl)retinamide [32], the vanilloids capsaicin and resiniferatoxin [34], and the rotenoid deguelin [20], presumably function as coenzyme Q antagonist to achieve their apoptogenic effects in transformed cells. Moreover, the closed or open conformation of the mitochondrial permeability transition pore complex is reportedly regulated by various coenzyme Q analogs that presumably stabilize or displace endogenous coenzyme Q, thereby regulating mitochondrial membrane permeability [35].

Figure 7. Mitochondrial bioenergetics confers sensitivity to TFN-induced mitochondrial disruption in premalignant and malignant prostate epithelial cells. (A) The PWR-1E cells were exposed for 6 hours to 50, 100, or 200 μM TFN or to an equal volume of the vehicle Me_2SO (control). The dissipation of $\Delta\Psi_m$ and enhanced ROS production were determined by concurrent staining with 40 nM $DiOC_6(3)$ and 5 μM dihydroethidium followed by cytofluorometric analysis. (B) An immunoblot assessment of cytosolic cytochrome *c* in permeabilized PWR-1E cells after a 12-hour exposure to 50, 100, or 200 μM TFN or to an equal volume of the vehicle Me_2SO (control). (C) The DIC images of DU-145 cells treated for 12 hours with Me_2SO (control) or 200 μM TFN. After treatment, the cells were stained with $DiOC_6(3)$ and dihydroethidium as described in panel (A) followed by cytofluorometric analysis. The results of this analysis are presented in the inset figures. Scale bars, 18 μm. (D) The DU-145 ρ^0 clones were exposed for 12 hours to 200 μM TFN or to an equal volume of the vehicle Me_2SO (control), stained, and analyzed by flow cytometry as described in panel (A).

A sharp decrease in the retention of the cationic probe $DiOC_6(3)$ that is accompanied by the oxidation of dihydroethidium to ethidium can be used to monitor catastrophic mitochondrial disruption in intact cells [20]. The control PWR-1E cells were gated, assuming they exhibited high $DiOC_6(3)$ fluorescence and low ethidium fluorescence. A 6-hour exposure to 50 or 100 μM TFN did not mediate a marked shift in the fluorescence intensity of either $DiOC_6(3)$ or ethidium in the sample populations. However, 200 μM TFN produced an obvious loss of $DiOC_6(3)$ fluorescence in approximately 50% of the treatment population accompanied by an increase in ethidium fluorescence in almost half of these cells (Figure 7*A*). Furthermore, a 12-hour exposure to 200 μM TFN caused an obvious increase in cytosolic cytochrome *c* in the PWR-1E cells relative to the lower concentrations of TFN or the Me_2SO-treated control cells (Figure 7*B*). Together, these results illustrated that 200 μM TFN caused a catastrophic disruption of the mitochondria in the PWR-1E cells sufficient to release cytochrome *c* from the mitochondrial intermembrane space.

We examined oxygen consumption by the PWR-1E cells exposed to 50, 100, and 200 μM TFN for 6 hours. The 50- and 100-μM treatments produced a roughly 29% to 33% suppression in oxygen consumption, respectively, compared with the Me_2SO-treated control cells (not shown), which was essentially similar to the suppression of oxygen consumption detected in these cells after the 4-hour exposure to 50 μM TFN (Figure 3*A*). Interestingly, the 6-hour exposure to 200 μM TFN promoted an increase in oxygen consumption in these cells that measured 7.95 ± 0.44 nmol of O_2/min/10^6 cells compared with 6.12 ± 0.09 nmol of O_2/min/10^6 cells in the Me_2SO-treated control cells (not shown). This increase in oxygen consumption could have been related to the induction of ROS production triggered by the 6-hour exposure to 200 μM TFN (Figure 7*A*) because enhanced ROS production reportedly increased oxygen consumption in isolated mitochondria that were triggered to undergo the mitochondrial permeability transition [36].

We repeated the flow cytometry assay using the DU-145 cells. A 6-hour exposure to 200 μM TFN shifted approximately 18% of the treatment population to low $DiOC_6(3)$ fluorescence intensity but did not markedly influence the fluorescence intensity of ethidium (not shown). After a 12-hour exposure, we could detect cytoplasmic vacuolizations in many of the DU-145 cells, and there was evidence of cell shrinkage and cell rounding (Figure 7*C*). Furthermore, roughly 55% of the treatment population had shifted to low $DiOC_6(3)$ fluorescence, and approximately 24% of these cells exhibited high ethidium fluorescence compared with the control cells (Figure 7*C*, *insets*). These biochemical effects were absent in the ρ^0 clones exposed to 200 μM TFN for 12 hours (Figure 7*D*), and we did not detect any visual signs of cytotoxicity in these cells during a 3-day exposure to 200 μM TFN (not shown). These results further demonstrated that a high *in vitro* dose (i.e., 200 μM) of TFN could promote a profound disturbance of mitochondrial function sufficient to cause mitochondrial permeabilization in the respiring cells.

Considering its presumed redox silent quality [5], and the fact that relatively high concentrations (i.e., ≥100 μM) of TFN diminished

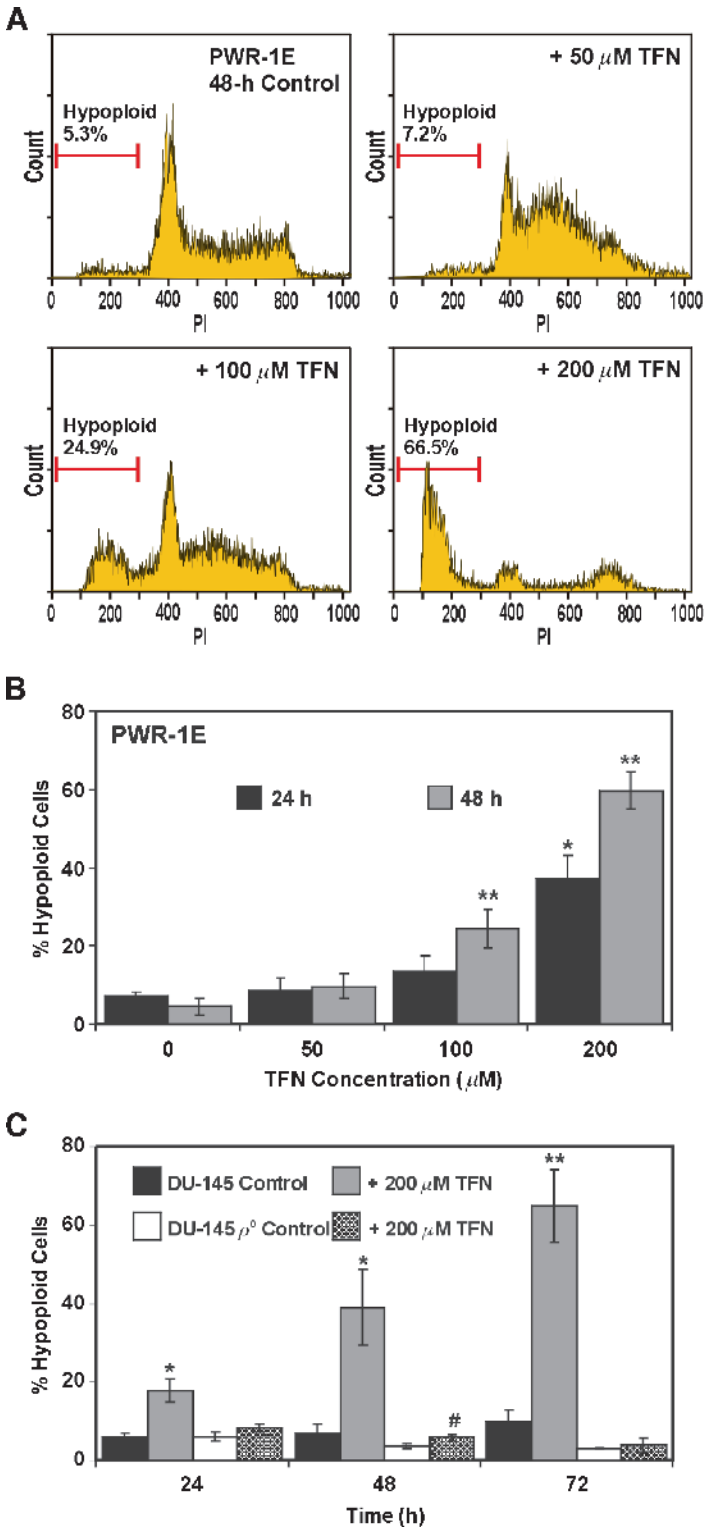

Figure 8. DU-145 uridine auxotrophs are markedly resistant to TFN-induced apoptosis. (A) Representative PI (DNA) histograms for PWR-1E cells exposed to Me_2SO (control) or to 50, 100, or 200 μM TFN for 48 hours. The gated cells detected below approximately 300 fluorescence units of PI on the linear *x*-axis of the representative histograms are designated the hypoploid apoptotic cell population. (B) A summary of the hypoploid PWR-1E cells observed after the 24- or 48-hour treatments described in panel (A). $^*P < .01$ compared with the 24-hour control; $^{**}P < .01$ compared with the 48-hour control. (C) The parental DU-145 cells and their ρ^0 clones were treated for 24, 48, or 72 hours with 200 μM TFN or with an equal volume of the vehicle Me_2SO (control). $^*P < .01$ compared with the 24- or 48-hour DU-145 control; $^{\#}P < .05$ compared with the 48-hour DU-145 ρ^0 control; $^{**}P < .001$ compared with the 72-hour DU-145 control.

succinate and NADH oxidation in isolated rat liver, heart, and kidney mitochondria [6], we can only speculate that the exposure to 200 μM TFN interrupted the normal redox function of coenzyme Q, perhaps at a site or sites in the electron transport chain besides DHODH, to mediate coenzyme Q redox cycling and mitochondrial damage in the PWR-1E and DU-145 cells. We plan to investigate this hypothesis further in future studies.

The time-dependent difference in the sensitivity to TFN-induced mitochondrial disruption observed between the PWR-1E and DU-145 cells could be due to the differences in DHODH expression and/or the bioenergetic phenotypes of these cells. In addition, as we mentioned previously, TFN exhibits a high binding affinity for proteins [8]. Thus, it is also conceivable that the 2% FBS in the culture medium of the DU-145 cells modulated the acute cytotoxic effects of TFN.

We examined DNA fragmentation in the PWR-1E cells exposed to 50, 100, or 200 μM TFN for 24 or 48 hours and noted a dose- (Figure 8*A*) and time-dependent (Figure 8*B*) increase in hypoploid apoptotic cells. The 200-μM concentration of TFN was extremely effective in this regard. Similarly, the DU-145 cells exhibited a time-dependent increase in the number of hypoploid cells after treatment with 200 μM TFN (Figure 8*C*), albeit this effect required more time to manifest itself in approximately 50% or more of the treatment population compared with the PWR-1E cells. Uridine had no effect on TFN-induced cytotoxicity in the DU-145 cells. A mean value of approximately 46% hypoploid cells was detected in triplicate samples after a 48-hour exposure to 200 μM TFN and 25 μM uridine (not shown).

DNA fragmentation was conspicuously absent in the ρ^0 clones exposed to 200 μM TFN for up to 72 hours (Figure 8*C*), which further implicated *de novo* pyrimidine synthesis and mitochondrial bioenergetics as the primary targets for TFN-induced cytostasis and apoptosis in the PWR-1E and parental DU-145 cells. It may be difficult to achieve a predominately apoptotic response to TFN in transformed prostate epithelial cells *in vivo* because TFN tissue concentrations are typically lower than the average steady-state plasma concentrations of approximately 200 μM that are achieved in humans that routinely use leflunomide [9].

A heightened response to mitogens such as androgens and epidermal growth factor coupled with enhanced mitochondrial bioenergetics and ROS production can sustain anomalous proliferation in transformed prostate epithelial cells, which can constitute a mechanistic underpinning for prostate tumorigenesis. Given the likely collection of factors linked to prostate cancer development and the indolent nature of this disease, agents such as antiandrogens (e.g., 5-α-reductase inhibitors), anti-inflammatory agents (e.g., COX-2 inhibitors), and antioxidants (e.g., vitamin E) would emerge as logical contenders in the arena of prostate cancer chemoprevention [37]. However, to date, extensive mainstream success in this area of chemoprevention has not been achieved.

The noted lack of practical success in prostate cancer chemoprevention points to an urgent need to identify and characterize novel prostate cancer-chemopreventive agents. Mitogens drive the rapid cell expansion in normal lymphocytes, which can become mediators of chronic inflammatory diseases such as rheumatoid arthritis. Suppression of the *de novo* pathway for pyrimidine synthesis in mitogen-activated T cells is believed to be the principal mechanism of TFN with respect to its ability to alleviate the pathologic events associated with this disease [13]. Because prostate tumorigenesis is also associated with mitogenic, bioenergetic, and inflammatory triggers, we anticipated that TFN could be a unique candidate as a prostate cancer-chemopreventive agent. Our *in vitro* evaluations of TFN using premalignant and malignant prostate epithelial cells have shown that this agent promotes growth-inhibitory (i.e., cytostatic and apoptotic) as well as anti-inflammatory (e.g., antioxidant) anticancer effects in these cells through the modulation of *de novo* pyrimidine synthesis and mitochondrial bioenergetics. These multifactorial properties are indeed novel. We envision that our mechanistic evidence will warrant continued investigations of TFN, as well as *de novo* pyrimidine synthesis and mitochondrial bioenergetics, in the prevention of prostate cancer.

Acknowledgments

The authors thank Christine Childs of the University of Colorado Cancer Center Flow Cytometry Core for her assistance with the acquisition of the flow cytometry data presented in this study.

References

[1] Bettuzzi S, Brausi M, Rizzi F, Castagnetti G, Peracchia G, and Corti A (2006). Chemoprevention of human prostate cancer by oral administration of green tea catechins in volunteers with high-grade prostate intraepithelial neoplasia: a preliminary report from a one-year proof-of-principle study. *Cancer Res* **66**, 1234–1240.

[2] Sun SY, Hail N Jr, and Lotan R (2004). Apoptosis as a novel target for cancer chemoprevention. *J Natl Cancer Inst* **96**, 662–672.

[3] Costello LC, Franklin RB, and Feng P (2005). Mitochondrial function, zinc, and intermediary metabolism relationships in normal prostate and prostate cancer. *Mitochondrion* **5**, 143–153.

[4] Evans DR and Guy HI (2004). Mammalian pyrimidine biosynthesis: fresh insights into an ancient pathway. *J Biol Chem* **279**, 33035–33038.

[5] Davis JP, Cain GA, Pitts WJ, Magolda RL, and Copeland RA (1996). The immunosuppressive metabolite of leflunomide is a potent inhibitor of human dihydroorotate dehydrogenase. *Biochemistry* **35**, 1270–1273.

[6] Jöckel J, Wendt B, and Löffler M (1998). Structural and functional comparison of agents interfering with dihydroorotate, succinate and NADH oxidation of rat liver mitochondria. *Biochem Pharmacol* **56**, 1053–1060.

[7] Tallantyre E, Evangelou N, and Constantinescu CS (2008). Spotlight on teriflunomide. *Int MS J* **15**, 62–68.

[8] Breedveld FC and Dayer JM (2000). Leflunomide: mode of action in the treatment of rheumatoid arthritis. *Ann Rheum Dis* **59**, 841–849.

[9] Rozman B (2002). Clinical pharmacokinetics of leflunomide. *Clin Pharmacokinet* **41**, 421–430.

[10] Kalden JR, Schattenkirchner M, Sörensen H, Emery P, Deighton C, Rozman B, and Breedveld F (2003). The efficacy and safety of leflunomide in patients with active rheumatoid arthritis: a five-year follow up study. *Arthritis Rheum* **48**, 1513–1520.

[11] Shawver LK, Schwartz DP, Mann E, Chen H, Tsai J, Chu L, Taylorson L, Longhi M, Meredith S, Germain L, et al. (1997). Inhibition of platelet-derived growth factor–mediated signal transduction and tumor growth by *N*-[4-(trifluoromethyl)-phenyl] 5-methylisoxazole-4-carboxamide. *Clin Cancer Res* **3**, 1167–1177.

[12] Baumann P, Mandl-Weber S, Volkl A, Adam C, Bumeder I, Oduncu F, and Schmidmaier R (2009). Dihydroorotate dehydrogenase inhibitor A771726 (leflunomide) induces apoptosis and diminishes proliferation of multiple myeloma cells. *Mol Cancer Ther* **8**, 366–375.

[13] Rückemann K, Fairbanks LD, Carrey EA, Hawrylowicz CM, Richards DF, Kirschbaum B, and Simmonds HA (1998). Leflunomide inhibits pyrimidine *de novo* synthesis in mitogen-stimulated T-lymphocytes from healthy humans. *J Biol Chem* **273**, 21682–21691.

[14] Sawamukai N, Saito K, Yamaoka K, Nakayamada S, Ra C, and Tanaka Y (2007). Leflunomide inhibits PDK1/Akt pathway and induces apoptosis of human mast cells. *J Immunol* **179**, 6479–6484.

[15] Xu X, Williams JW, Gong H, Finnegan A, and Chong AS (1996). Two activities of the immunosuppressive metabolite of leflunomide, A77 1726. Inhibition of pyrimidine nucleotide synthesis and protein tyrosine phosphorylation. *Biochem Pharmacol* **52**, 526–534.

[16] Webber MM, Bello D, Kleinman HK, Wartinger DD, Williams DE, and Rhim JS (1996). Prostate specific antigen and androgen receptor induction and characterization of an immortalized adult human prostatic epithelial cell line. *Carcinogenesis* **17**, 1641–1646.

[17] Sun S-Y, Yue P, and Lotan R (1999). Induction of apoptosis by *N*-(4-hydroxyphenyl) retinamide and its association with reactive oxygen species, nuclear retinoic acid receptors, and apoptosis related genes in human prostate carcinoma cells. *Mol Pharmacol* **55**, 403–410.

[18] Hail N Jr, Chen P, and Kepa JJ (2009). Selective apoptosis induction by the cancer chemopreventive agent *N*-(4-hydroxyphenyl)retinamide is achieved by modulating mitochondrial bioenergetics in premalignant and malignant human prostate epithelial cells. *Apoptosis* **14**, 449–863.

[19] Fletcher CV, Kawle SP, Kakuda TN, Anderson PL, Weller D, Bushman LR, Brundage RC, and Remmel RP (2000). Zidovudine triphosphate and lamivudine triphosphate concentration-response relationships in HIV-infected persons. *AIDS* **14**, 2137–2144.

[20] Hail N Jr and Lotan R (2004). Apoptosis induction by the natural product cancer chemopreventive agent deguelin is mediated through the inhibition of mitochondrial respiration. *Apoptosis* **9**, 437–447.

[21] Litvinov IV, Vander Griend DJ, Xu Y, Antony L, Dalrymple SL, and Isaacs JT (2006). Low-calcium serum-free defined medium selects for growth of normal prostatic epithelial stem cells. *Cancer Res* **66**, 8598–8607.

[22] Löffler M, Becker C, Wegerle E, and Schuster G (1996). Catalytic enzyme histochemistry and biochemical analysis of dihydroorotate dehydrogenase/oxidase and succinate dehydrogenase in mammalian tissues, cells and mitochondria. *Histochem Cell Biol* **105**, 119–128.

[23] Ripple MO, Henry WF, Rago RP, and Wilding G (1997). Prooxidant-antioxidant shift induced by androgen treatment of human prostate carcinoma cells. *J Natl Cancer Inst* **89**, 40–48.

[24] Higgins LH, Withers HG, Garbens A, Love HD, Magnoni L, Hayward SW, and Moyes CD (2009). Hypoxia and the metabolic phenotype of prostate cancer cells. *Biochim Biophys Acta* **1787**, 1433–1443.

[25] Ringshausen I, Oelsner M, Bogner C, Peschel C, and Decker T (2008). The immunomodulatory drug leflunomide inhibits cell cycle progression of B-CLL cells. *Leukemia* **22**, 635–638.

[26] López-Navarro AT, Bueno JD, Gil A, and Sánchez-Pozo A (1996). Morphological changes in hepatocytes of rats deprived of dietary nucleotides. *Br J Nutr* **76**, 579–589.

[27] Angermüller S and Löffler M (1996). Localization of dihydroorotate oxidase in myocardium and kidney cortex of the rat. An electron microscopic study using the cerium technique. *Histochem Cell Biol* **103**, 287–292.

[28] Venkataraman S, Jiang X, Weydert C, Zhang Y, Zhang HJ, Goswami PC, Ritchie JM, Oberley LW, and Buettner GR (2005). Manganese superoxide dismutase overexpression inhibits the growth of androgen-independent prostate cancer cells. *Oncogene* **24**, 77–89.

[29] Traut TW (1994). Physiological concentrations of purines and pyrimidines. *Mol Cell Biochem* **140**, 1–22.

[30] Peters GJ, Kraal I, and Pinedo HM (1992). *In vitro* and *in vivo* studies on the combination of brequinar sodium (DUP-785; NSC 368390) with 5-fluorouracil; effects of uridine. *Br J Cancer* **65**, 229–233.

[31] Rodríguez-Serrano F, Marchal JA, Ríos A, Martínez-Amat A, Boulaiz H, Prados J, Perán M, Caba O, Carrillo E, Hita F, et al. (2007). Exogenous nucleosides modulate proliferation of rat intestinal epithelial IEC-6 cells. *J Nutr* **137**, 879–884.

[32] Hail N Jr and Lotan R (2001). Mitochondrial respiration is uniquely associated with the prooxidant and apoptotic effects of *N*-(4-hydroxyphenyl)retinamide. *J Biol Chem* **276**, 45614–45621.

[33] Hail N Jr (2005). Mitochondria: a novel target for the chemoprevention of cancer. *Apoptosis* **10**, 687–705.

[34] Hail N Jr and Lotan R (2002). Examining the role of mitochondrial respiration in vanilloid-induced apoptosis. *J Natl Cancer Inst* **94**, 1281–1292.

[35] Fontaine E, Ichas F, and Bernardi P (1998). A ubiquinone-binding site regulates the mitochondrial permeability transition pore. *J Biol Chem* **273**, 25734–25740.

[36] Batandier C, Leverve X, and Fontaine E (2004). Opening of the mitochondrial permeability transition pore induces reactive oxygen species production at the level of the respiratory chain complex I. *J Biol Chem* **279**, 17197–17204.

[37] Thompson IM, Tangen CM, Goodman PJ, Lucia MS, and Klein EA (2009). Chemoprevention of prostate cancer. *J Urol* **182**, 499–507.